# Stable Kerr frequency combs excited in the vicinity of strong modal dispersion disruptions

Hossein Taheri[a], Anatoliy Savchenkov[a,*], and Andrey B. Matsko[b]

[a]Department of Electrical and Computer Engineering, University of California at Riverside, 900 University Ave., Riverside, California 92521, USA
[b]Jet Propulsion Laboratory, California Institute of Technology, 4800 Oak Grove Drive, Pasadena, CA 91109, USA

## ABSTRACT

Optical microresonators possessing Kerr-type nonlinearity have emerged over the past decade as reliable and versatile sources of optical frequency combs, with varied applications including in the generation of low-phase-noise radio frequency (RF) signals, small-footprint precision timekeeping, and LiDAR. One of the key parameters affecting Kerr microcomb generation in different wavelength ranges is cavity modal dispersion. Dispersion effects such as avoided mode crossings (AMCs) have been shown to greatly limit mode-locked microcomb generation, especially when pumping in close proximity to such disruptions. We present numerical modeling and experimental evidence demonstrating that using an auxiliary laser pump can suppress the detrimental impact of near-pump AMCs. We also report, for the first time to our knowledge, the possibility of the breaking of characteristic soliton steps into two stable branches corresponding to different stable pulse trains arising from the interplay of dichromatic pumping and AMCs. These findings bear significance, particularly for the generation of frequency combs in larger resonators or at smaller wavelengths, such as the visible range, where the cavities become overmoded.*

**Keywords:** Dissipative Kerr Solitons, High-Q Microresonators, Optical Frequency Combs, Soliton Crystals, Avoided Mode Crossings, Dual-frequency Pumping

## 1. INTRODUCTION

The generation of optical frequency combs in high-Q (quality factor) dielectric microresonators possessing Kerr nonlinearity by pumping the optical cavity with a continuous wave (CW) laser has been a vibrant and fruitful field of research over the past decade, resulting in promising demonstrations targeted at various applications, including low-phase noise microwave and radio frequency (RF) signal generation, light detection and ranging (LiDAR), spectroscopy, and timekeeping.[1,2] Such applications largely rely on the repeatable generation of stable frequency microcombs[3] and have been demonstrated in a variety of resonator geometries and material platforms in whispering gallery mode and photonic integrated resonators.[4] The impact on microcomb generation conditions and its spectrum of various physical parameters relating to the laser pump driving the cavity and the resonator enabling the emergence of sidebands for this excitation frequency have been explored. Among those, the dispersion profile of the desired resonator mode family being pumped was highlighted in early demonstrations[5] and dispersion engineering through resonator geometry was later exploited to achieve broadband microcombs.[6,7] It was also shown that microcomb soliton formation will not be possible when pumping the cavity near strong

*Present address: Jet Propulsion Laboratory, California Institute of Technology, 4800 Oak Grove Drive, Pasadena, CA 91109, USA
Send correspondence to H. Taheri: hossein.taheri@ucr.edu
*This article is published as:* Hossein Taheri, Anatoliy Savchenkov, and Andrey B. Matsko "Stable Kerr frequency combs excited in the vicinity of strong modal dispersion disruptions," Proc. SPIE 12407, Laser Resonators, Microresonators, and Beam Control XXV, 1240709 (15 March 2023); https://doi.org/10.1117/12.2652926.

modal profile disruptions caused by avoided mode crossings (AMCs), also called mode anti-crossings,[8] where the overlap between the optical frequencies and spatial mode profiles of the pumped mode family and a crossing mode family creates a means of channeling power from the former to the latter.[9] This problem will be more pronounced in larger microresonators, which are of interest, e.g., for accessing smaller (few GHz) repetition rates, and at smaller wavelengths such as the visible range, where cavities become highly overmoded[10]

While the mainstream research in the Kerr microcomb community has focused on CW pumping, more recently attention has also been paid to driving the resonator with what could be called "temporally structured light." Examples include microcomb generation and soliton formation in both the normal and anomalous dispersion regimes by a modulated pump[11–17] and synchronous driving by pump modulation and pulse shaping.[18] An excitation scheme, which from the perspective of the number of frequency sidebands of the pump driving the cavity could be considered a limiting case, is dual-frequency or dichromatic pumping.[19–21] An advantage of dichromatic pumping is that the frequencies of the two laser pumps could in principle be arbitrarily large, while sideband generation by the intensity or phase modulation of a CW laser for subsequent pulse shaping would require prohibitively fast modulators at the typical free spectral ranges (FSRs) of cavities utilized for microcomb generation (tens of GHz up to roughly 1 THz). We will present here a systematic study of the dual-frequency pumping of a Kerr microcavity near AMCs with the goal of answering the following question: Can dichromatic pumping counter the detrimental impact of near-pump AMCs and enable soliton microcomb generation? We will present numerical modeling and experimental results to shed some light on this problem of practical significance.

## 2. OVERVIEW OF DUAL-FREQUENCY PUMPING

Dual-frequency pumping can be used to fix the two degrees of freedom of a microcomb (center frequency and repetition rate) by transferring the stability of the two pumps to the microcomb they excite.[21–23] The pumps can be locked to two external frequency references such as two atomic transitions. When the pump frequencies are more than one FSR apart, the phase noise of the microcomb repetition rate will be reduced as a result of frequency division by the square of the ratio of the pumps beatnote over the repetition rate; see Fig. 4(b) in Taheri *et al.*[24] for experimental evidence, and the section titled "Phase noise reduction of the RF beatnote" in Taheri *et al.*[16] for an expression relating the phase noise of the generated subharmonic (microcomb repetition rate) to that of pumps beatnote and of a Kerr microcomb driven by a free-running laser.

Before proceeding to the results, we note that dichromatic pumping has been explored theoretically and experimentally with other applications in mind, such as for random number generation using a degenerate optical parametric oscillator,[25,26] optical soliton memories and buffers,[20] extending microcomb bandwidth,[27,28] so-called synthetic (or synthesized) soliton crystals,[21,29] photonic dissipative discrete time crystals,[23,24,30,31] and low-threshold Kerr solitons.[32] It should be noted that like many other concepts in Kerr microcomb research, dual-frequency pumping has also been studied in the context of fibers[33] and fiber cavities.[34]

While the realization of dissipative discrete time crystals in a dichromatically pumped Kerr microcavity relies on subharmonic generation,[24,31] the synthesized soliton crystals demonstrated by Lu *et al.*[29] (and similar microcombs reported by Strekalov and Yu[19]) are microcombs based on the four-wave mixing of the two driving lasers so that the repetition rate exactly matches the beatnote of the pumps. In the time domain, the latter type of microcombs corresponds to pulse trains in which every single potential lattice trap site is occupied by a soliton pulse to form a "perfect" soliton crystal with no missing pulse peaks in the beatnote-defined modulation pattern of the CW background. Looking at the frequency spectrum $\tilde{\psi}_m$ ($m$ being the relative mode number, $m \in \{0, \pm1, \pm2, \dots\}$) of a soliton pulse train $\psi(\theta)$ and exploiting the linear shift property of the Fourier transform,

$$\psi(\theta - 2\pi k/N) \overset{\mathcal{F}}{\longleftrightarrow} \tilde{\psi}_m \, \mathrm{e}^{\mathrm{i}m\cdot 2\pi k/N},$$

one can readily show that for such a synthetic perfect soliton crystal with $N$ equidistant solitons per cavity round-trip time (and disregarding the impact of the CW background), the power of the center comb line ($m = 0$) will roughly equal $N^2|\tilde{\psi}_0|^2$, scaling as $N^2$; see Fig. 3 in Lu *et al.*[29]

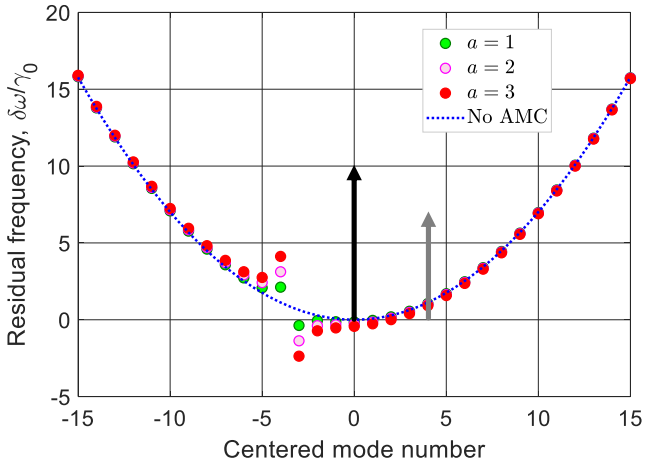


Figure 1. The residual or integrated dispersion profile of the cavity considered in the systematic study of the impact of avoided mode crossings (AMCs) on soliton microcomb generation with one and two pumps. The dotted blue curve is the residual frequency in the absence of AMCs (i.e., ideal anomalous group velocity dispersion). An AMC added at $b_{\mathrm{AMC}} = -4$ with increasing intensity $a_{\mathrm{AMC}} = 1, 2, 3$ is studied.

## 3. SYSTEMATIC STUDY OF DICHROMATIC PUMPING NEAR MODE ANTI-CROSSINGS

In this study, we exploit the generic formulation presented in Taheri *et al.*[21] for the dual-frequency pumping of one modal family in a Kerr microcavity. To include the impact of AMCs in the dispersion profile, we utilize a two-parameter model of mode anti-crossings,[8]

$$\omega_\eta = \omega_0 + D_1\eta + \frac{1}{2}D_2\eta^2 + \frac{a_{\mathrm{AMC}}/2}{\eta - 1/2 - b_{\mathrm{AMC}}} \tag{1}$$

where $a_{\mathrm{AMC}}$ signifies the strengths of the AMC disruption, $b_{\mathrm{AMC}}$ determines its spectral position with respect to the mode number labeled 0 (centered or relative mode number), $\omega_\eta$ refers to the resonance frequency of the cavity mode with relative mode number $\eta$, $D_1/2\pi$ is the cavity FSR in Hz at the center mode $\omega_0$, and $D_2 = \omega_1 - 2\omega_0 + \omega_{-1}$ is the 2nd-order dispersion coefficient of the unperturbed pumped mode family. Starting with an anomalous group velocity dispersion profile with residual or integrated dispersion profile $\delta\omega = \omega_\eta - \omega_0 - D_1\eta$ plotted in Fig. 1 (dotted blue line, normalized to the cavity half-width at half-maximum $\gamma_0$), an AMC is added close to the main pump (longer, black, arrow) and its strengths is gradually increased ($b_{\mathrm{AMC}} = -4$ and $a_{\mathrm{AMC}} = 1, 2, 3$). In each case, soliton microcomb generation with dichromatic pumping is investigated.

We first consider the case where the second pump drives the cavity with smaller power compared to the first one and on the opposite spectral side as the AMC at different modes (2, 3, and 4 FSRs away from the other pump). Note that beyond ease of referencing, the labeling of the two pumps as the first or the second is arbitrary and does not correlate with the pump being stronger or not. (A different configuration of the pumps presented in a subsequent section will further highlight this notion.) Indeed the two pumps have comparable powers and, as the results will show, the presence of both gives rise to the emergence of solitons. This is in contrast to the case where one pump generates a soliton microcomb and then a second pump with smaller power is introduced to coherently lock to this frequency comb. The power of the weaker pump is chosen to be slightly sub-threshold (e.g., $0.98 < 1$ in normalized units, where the normalization follows those of the standard LLE, Lugiato-Lefever equation, in Kerr microcomb research[35]) and that of the stronger pump to be above the nonlinear sideband generation threshold (1.4 and 1.5) but not by a lot. Monochromatic pumping of the cavity with either pump cannot independently create soliton microcombs except over a small range of pump-resonance detuning values, as can be seen in the steady-state power vs. detuning curve of Fig. 2(a). Every data point in Fig. 2 and subsequent similar comb energy vs. detuning curves corresponds to one run of the LLE from random

initial conditions (hard excitation) for tens of cavity photon lifetimes, till steady states (if achievable) prevailed. In Fig. 2(a), the so-called soliton steps indicating the generation of different numbers of soliton peaks per cavity round-trip time are visibly seen, albeit in a very narrow region between normalized detuning values of 1.4 and 2.7 (detuning normalized to $-\gamma_0$, following Chembo and Menyuk[35]). When an AMC with $a_{\mathrm{AMC}} = 1$ is added at $b_{\mathrm{AMC}} = -4$, the situation is further degraded and some of the steps show signs of destabilization, as indicated by the narrowing of the steps and the appearance of blobs of data points because of random comb powers at the end of the numerical simulation run; Fig. 2(b).

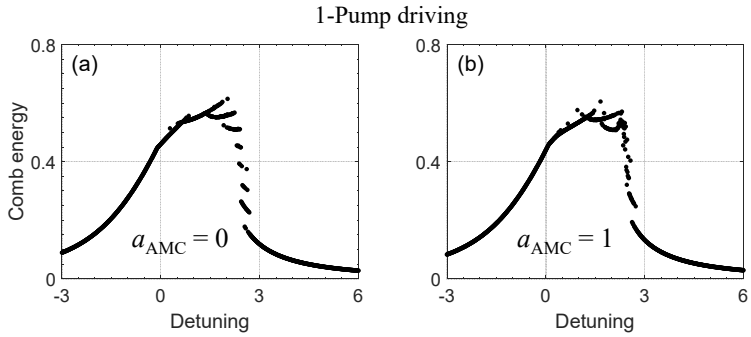


Figure 2. Steady-state comb energy vs. normalized detuning for a monochromatically pumped Kerr cavity (a) without and (b) with near-pump modal dispersion disruption. Comb energy is normalized by the power of the pump. Every data point corresponds to one run of the Lugiato-Lefever equation from random initial conditions till steady states (if achievable) prevailed. (a) Case of ideal anomalous dispersion (no mode anti-crossings), corresponding to the blue dotted line in Fig. 1. The so-called soliton steps indicate the generation of different numbers of soliton peaks per cavity round-trip time in a very narrow region. (b) When an avoided mode crossing (AMC) with $a_{\mathrm{AMC}} = 1$ is added at $b_{\mathrm{AMC}} = -4$ (green data points in Fig. 1), soliton formation regime narrows and some of the soliton steps show signs of destabilization.

We now add another pump to the picture and repeat the study now with dichromatic pumping where the two pump frequencies are 4 FSRs apart. The results are plotted in Fig. 3. For an ideal anomalous dispersion profile, Fig. 3(a), 4 clear soliton steps are observed in the comb energy vs. detuning curve. Compared to Fig. 2(a), a much wider region of the comb energy vs. detuning plane now supports soliton formation. Additionally, as highlighted earlier in the literature,[12,21,36] because of the pumps beatnote-induced crystallization and trapping effect of the CW background on which solitons sit, the number of soliton peaks per cavity round-trip time is now fixed by the beatnote of the pumps (number of FSRs separating them), here 4 solitons steps, which is different from what was observed when pumping monochromatically (at least 7 steps are discernible in Fig. 2(a) – the lowest-energy level does not signify soliton formation).

With an AMC characterized by $a_{\mathrm{AMC}} = 1$ and $b_{\mathrm{AMC}} = -4$ added to the dispersion profile, Fig. 3(b), the previously observed 4 soliton steps are still present, but the top-most or highest-energy step becomes partially blurry, signifying the destabilization of some of the soliton trains which were stable in the absence of modal disruptions. As the AMC grows stronger, lower-energy soliton steps too reveal signs of destabilization, starting from smaller detuning values where temporal pulse widths are longer; Fig. 3(c). As the strengths of the AMCs grows even further, it naturally overpowers the cavity drive and dominates, prohibiting soliton microcomb generation, Fig. 3(d).

## 4. DISCUSSION

The top-most soliton step in the example summarized in Fig. 3 signifies microcombs with frequency harmonics which are 4 FSRs aways, i.e., "perfect" soliton crystals created by the four-wave mixing of the pumps and without subharmonic generation.[19,29] Therefore, destabilization of this step in Fig. 3(b) hints at the deviation of the microcomb spectrum from the perfect soliton crystal comprising 4 equally-spaced solitons per cavity round-trip time through the excitation of subharmnonics (comb teeth between the pumps), or equivalently, by the reduction of the number of solitons peaks from the maximum dictated by the beatnote of the pumps (4 in this case). It should be noted that the deviation of the soliton train from the perfect soliton crystal could in principle occur

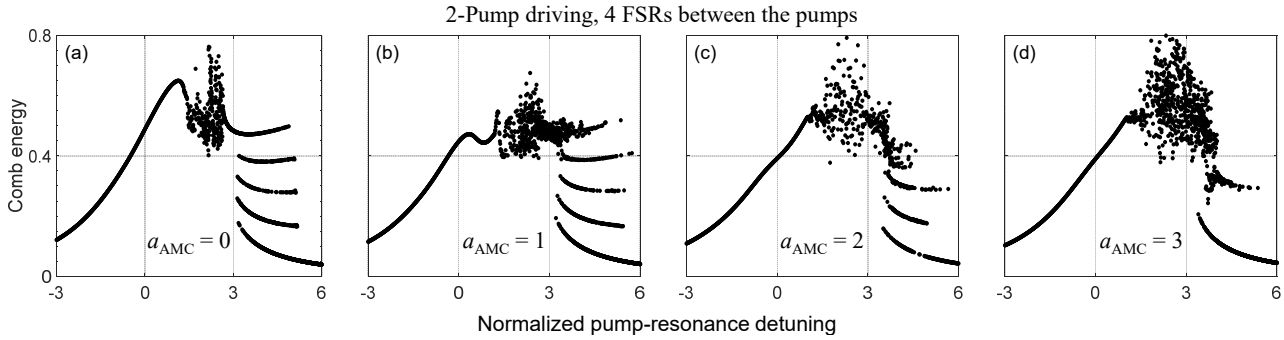


Figure 3. Steady-state comb energy vs. normalized detuning for a dichromatically pumped Kerr cavity (a) without and (b-d) with near-pump modal dispersion disruption. Comb energy is normalized by the power of the pump exciting the $\omega_0$ resonance. An avoided mode crossing (AMC) is added at $b_{\mathrm{AMC}} = -4$ with increasing strength (b) $a_{\mathrm{AMC}} = 1$, (c) $a_{\mathrm{AMC}} = 2$, and (d) $a_{\mathrm{AMC}} = 3$. Normalized pump intensities are 1.4 and 0.98, and comb energy is normalized to the power of the pump driving the center mode.

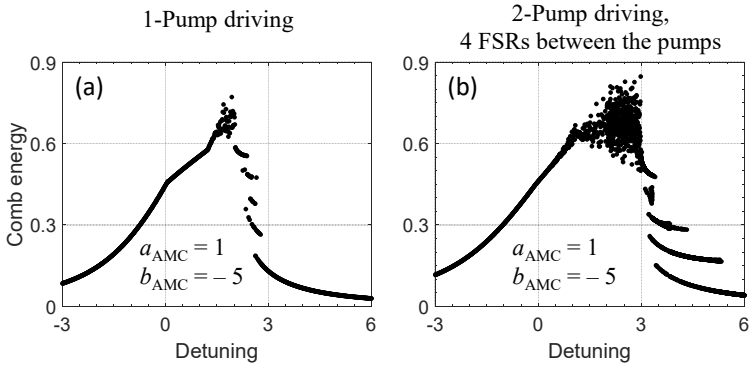


Figure 4. Steady-state comb energy vs. normalized detuning for (a) a monochromatically- and (b) a dichromatically-pumped Kerr cavity with an avoided mode crossing (AMC) at $b_{\mathrm{AMC}} = -5$ with strength $a_{\mathrm{AMC}} = 1$. In (b) the pumps are 4 FSRs away. Four soliton steps and the destabilization of the highest-energy soliton steps are observed, essentially following the same trend as in Fig. 3.

also by a non-uniform distribution of the maximum number of pulse peaks around the cavity allowed by the pumps beatnote, as will be seen in the next section. In this case, subharmonics will again emerge.

Upon closer examination, it is seen that for $a_{\mathrm{AMC}} = 3$ and $b_{\mathrm{AMC}} = -4$ in Fig. 3(d), the second soliton step, corresponding to 2 solitons per cavity round-trip time, survives the other soliton steps (especially the lower-energy single-soliton step). This observation could be attributed to the specific choice of parameters in this example (i.e., the weaker pump added 4 FSRs from the stronger pump and mirroring the mode anti-crossing 4 FSRs on the lower-frequency side), in the sense that frequency pinning by the AMC on the left and the presence of the second pump on the right (Fig. 1) reinforce a potential lattice trap which prefers two-soliton states.

The study presented above suggests that dichromatic pumping can enable soliton microcomb generation in a parameter range where AMCs prohibit their appearance. When the AMC becomes too strong, it then naturally dominates again, prohibiting the generation of solitons. We repeated the same exercise with pumps beatnotes equaling 3 and 2 FSRs for a similar AMC-induced dispersion disruption at $b_{\mathrm{AMC}} = -4$ with increasing intensities of $a_{\mathrm{AMC}} = 1, 2, 3$ and observed the same trend. An AMC at $b_{\mathrm{AMC}} = -5$, Fig. 4 confirmed these findings as well.

## 5. EMERGENCE OF A PAIR OF BISTABLE SOLITON BRANCHES

We performed a similar analysis for a different configuration of the pumps, namely the case where the pumps schematically shown in Fig. 1 are swapped so that the stronger pump is separated by a larger frequency from the mode crossing. The cavity dispersion profile is the same as the green curve in Fig. 1, with an AMC characterized by $b_{\mathrm{AMC}} = -4$ and $a_{\mathrm{AMC}} = 1$. While this analysis confirms the previously stated general conclusion regarding

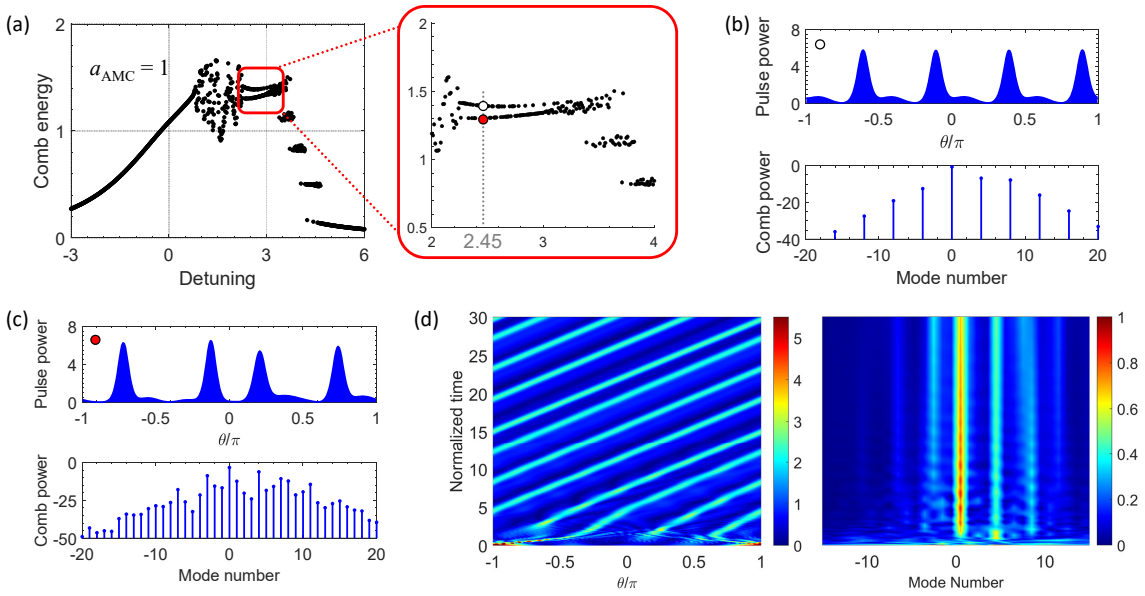


Figure 5. Branching of a soliton step when the cavity is dichromatically pumped in the vicinity of a modal dispersion disruption; c.f. Fig. 3(b). The dispersion profile is similar to the green curve in Fig. 1. The two pumps are, however, swapped compared to what is schematically shown in Fig. 1 so that the stronger pump is separated by a larger frequency from the mode crossing frequency. (b) The pulse waveform per round-trip time (upper panel) and microcomb spectrum (lower panel) corresponding to the higher-energy state at the normalized detuning value marked by the vertical dotted line (white circle) in the inset of (a). (c) Same as (b) for the lower-energy state marked by the red circle in the inset of (a). (d) Stable pulse propagation (left panel) and comb spectrum evolution (right panel) for the microcomb depicted in (c) over tens of cavity photon lifetimes. This microcomb was excited by noisy pumps, verifying that the lower-energy branch is stable.

the advantage of dichromatic pumping near an AMC, it interestingly also reveals *a pair of bistable soliton states* which we discuss briefly in this section; Fig. 5.

As seen in Fig. 5(a), the top-most soliton step breaks into two branches; see the inset. The pulse waveform per round-trip time (upper panel) and microcomb spectrum (lower panel) corresponding to each branch at the normalized detuning value marked by the vertical dotted line in the inset of Fig. 5(a) are illustrated in Fig. 5(b,c). Figure 5(b) depicts the "perfect" soliton crystal corresponding to the higher-energy branch (white circle) and Fig. 5(c) shows the pulse train corresponding to the lower-energy branch (red circle). The latter differs from the former in that the four pulses exiting the cavity per each round-trip time are not equally spaced from each other; one of the pulses huddles closer to another pulse, this deviation from the perfect crystallization of the solitons resulting in the appearance of subharmonics between the pumps. Additionally, this pulse appears weaker (has a smaller peak power) compared to the other three and each pulse in Fig. 5(b) (the upper branch).

By adding intensity and phase noise to both pumps, we verified that the lower-energy branch is stable. Figure 5(d) demonstrates stable pulse propagation (left panel) and comb spectrum evolution (right panel) for the microcomb of Fig. 5(c) over tens of cavity photon lifetimes. This microcomb was excited by noisy pumps with added random fluctuations chosen from a uniform distribution through hard excitation (i.e., a high-energy random initial condition).

## 6. EXPERIMENTAL EVIDENCE

Experimental evidence supporting the above conclusions regarding the impact of dichromatic pumping near AMCs can be seen in Figs. 6, and in previously published data, as briefly discussed below.

A magnesium fluoride whispering gallery mode (WGM) cavity was used to obtain the data plotted in Fig. 6. Here monochromatic pumping of the WGM resonator does excite a stable microcomb. The pump is self-injection-locked to the pumped cavity mode. The microcomb spectrum, however, is not clean and the envelope deviates

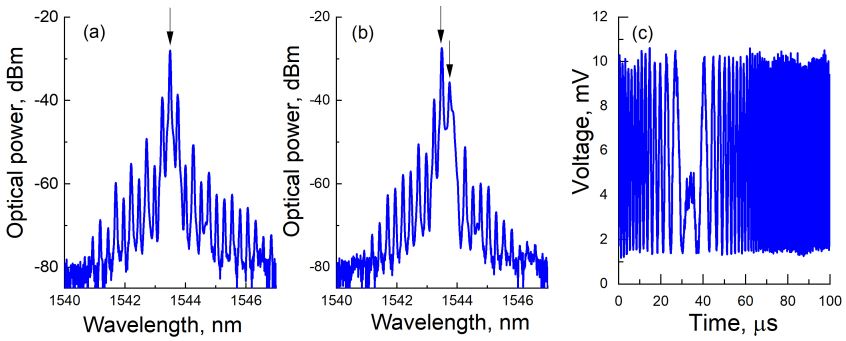


Figure 6. Experimental data for dichromatic pumping of a magnesium fluoride cavity pumped by (a) a distributed feedback (DFB) laser and generating a stable microcomb, and by (b) two lasers, one DFB laser (left black arrow) and one free-running fiber laser (right black arrow). In both cases, the DFB laser is self-injection-locked to the cavity mode it excites. In (b), the second pump is swept in the vicinity of the first sideband of the DFB laser pump (1 FSR separating the two pumps) till it locked to the microcomb excited by the latter. Comparison of (a) and (b) shows that the presence of both pumps has significantly changed the microcomb spectral envelope, indicating their dominating impact in the presence of resonator dispersion irregularities. (c) The beatnote of the fiber laser and its nearest microcomb harmonic, recorded on a slow photodiode, as the frequency of the fiber laser is scanned. The quiet region near 55 $\mu$s signifies the coherent locking of the fiber laser to the microcomb, as predicted previously.[21,23]

from a hyperbolic secant, indicating that the pulse shape is not solitonic; Fig. 6(a). Addition of another pump (a free-running fiber laser), however, notably changes the microcomb envelope, hinting at the irregular dispersion being partially suppressed by dual-frequency driving; Fig. 6(b). In this experiment, the fiber laser and the DFB laser frequencies were chosen to be only one FSR apart. The locking of the fiber laser to the microcomb was verified by monitoring the beatnote between this laser and its adjacent comb sideband (microcomb sideband labeled -1 in the notation adopted in the previous sections) on a (slow) photodiode; the quiet region near 55 microsecond sweep time in Fig. 6(c) indicates the locking range predicted and found numerically earlier.[21] We have reported elsewhere[37] that modulation of the fiber laser at a frequency slightly off the repetition rate of the microcomb excited by the DFB laser results in the observation of independent optical and RF locking ranges.

Another example of the dominant impact of dichromatic pumping near AMCs can be seen in Supplementary Figures 1 and 2 in Taheri *et al.*,[24] where two distributed feedback (DFB) lasers were self-injection-locked to two different modes of the same modal family of a magnesium fluoride WGM resonator. Pumping the cavity with one DFB laser did not result in microcomb generation in the frequency window of interest around 1545 nm. When the pumps excited four-wave mixing sidebands without subharmonic generation and created a "perfect" soliton crystal, Supplementary Figures 1,[24] the comb envelope did not reveal strong signatures of AMC-induced irregularities in the microcomb spectrum. On the other hand, when the two pump frequencies were separated by 2 FSRs and a harmonics was excited between the two lasers, Supplementary Figure 2(e,f),[24] the comb envelope was not solitonic, revealing dispersion disruptions. Despite disruptions in the mode profile, however, a stable microcomb was generated. This was verified through monitoring the phase noise of the RF signal resulting from the demodulation of the microcomb repetition rate on a fast photodiode and ensuring it is a narrow signal hence indicating a quite comb; see Fig. 4(b) in the main text in Taheri *et al.*[24] It should be emphasized that even though the spectral envelopes of the microcombs were not exactly sech(·)-shaped for pumps beatnotes equaling 3 and 4 FSRs [Figs. 4(c,f) in the main text in Taheri *et al.*[24]], the generation of stable microcombs in a frequency range where monochromatic pumping could not generate microcombs demonstrated that dichromatic pumping had dominated the AMCs, giving rise to regular pulses.

Finally, we would like to highlight the measured dispersion profile in Supplementary Figure 1(c) of Lu *et al.*[29] There are missing data points in the integrated dispersion data near the center (mode number 0). However, traces of mode crossings very close to mode number 0 are evident in the existing data points. Despite this near-pump mode disruption, soliton microcomb generation was made possible through dual-frequency pumping in this work; see Fig. 1(c) of the main text in Lu *et al.*[29]

## 7. CONCLUSION

We reported a systematic study of the dichromatic pumping of a Kerr microcavity in close proximity of a modal dispersion disruption caused by an avoided mode crossing (AMC or mode anti-crossing). In a parameter regime where monochromatic pumping of the cavity near an AMC cannot generate stable frequency combs, dichromatic pumping can counter the prohibitive role of the AMC, creating stable soliton microcombs. Naturally, as AMCs grow stronger, they ultimately dominate again and avoid stable microcomb generation. Pulse trains with higher energy (those with more solitons per round-trip time) at smaller detunings (where the temporal duration of pulses is longer) are found to be more vulnerable to AMCs because solitons in such microcombs are more likely to interact with their neighboring pulses. We also found that the interplay of AMC and dual-frequency driving can in some pump configurations result in the breaking of soliton steps into two stable branches. To the best of our knowledge, this is the first observation of this type of stable microcombs. These results are important especially for the generation of stable and tunable frequency tones at previously unexplored wavelength windows, excitation of microcombs in smaller wavelengths (e.g., in the visible), and realization of few-GHz optical microcomb-based RF and microwave signal sources.

## 8. ACKNOWLEDGMENTS

The research performed by A.B.M was carried out at the Jet Propulsion Laboratory, California Institute of Technology, under a contract with the National Aeronautics and Space Administration, NASA (80NM0018D0004). H.T. acknowledges financial support by the National Science Foundation of the United States of America (NSF) and by NASA's Jet propulsion Laboratory.

## REFERENCES

[1] Pasquazi, A., Peccianti, M., Razzari, L., Moss, D. J., Coen, S., Erkintalo, M., Chembo, Y. K., Hansson, T., Wabnitz, S., Del'Haye, P., Xue, X., Weiner, A. M., and Morandotti, R., "Micro-combs: A novel generation of optical sources," *Physics Reports* **729**, 1–81 (Jan. 2018).

[2] Kippenberg, T. J., Gaeta, A. L., Lipson, M., and Gorodetsky, M. L., "Dissipative Kerr solitons in optical microresonators," *Science* **361**(6402), eaan8083 (2018).

[3] Udem, T., Holzwarth, R., and Hänsch, T. W., "Optical frequency metrology," *Nature* **416**, 233–237 (Mar. 2002).

[4] Kovach, A., Chen, D., He, J., Choi, H., Dogan, A. H., Ghasemkhani, M., Taheri, H., and Armani, A. M., "Emerging material systems for integrated optical Kerr frequency combs," *Adv. Opt. Photon.* **12**, 135–222 (Mar 2020).

[5] Del'Haye, P., Schliesser, A., Arcizet, O., Wilken, T., Holzwarth, R., and Kippenberg, T., "Optical frequency comb generation from a monolithic microresonator," *Nature* **450**(7173), 1214–1217 (2007).

[6] Brasch, V., Geiselmann, M., Herr, T., Lihachev, G., Pfeiffer, M. H. P., Gorodetsky, M. L., and Kippenberg, T. J., "Photonic chip–based optical frequency comb using soliton Cherenkov radiation," *Science* **351**, 357–360 (Jan. 2016).

[7] Bao, C., Taheri, H., Zhang, L., Matsko, A., Yan, Y., Liao, P., Maleki, L., and Willner, A., "High-order dispersion in Kerr comb oscillators," *JOSA B* **34**(4), 715–725 (2017).

[8] Herr, T., Brasch, V., Jost, J. D., Mirgorodskiy, I., Lihachev, G., Gorodetsky, M. L., and Kippenberg, T. J., "Mode spectrum and temporal soliton formation in optical microresonators," *Phys. Rev. Lett.* **113**, 123901 (Sep 2014).

[9] Matsko, A., Liang, W., Savchenkov, A., Eliyahu, D., and Maleki, L., "Optical Cherenkov radiation in overmoded microresonators," *Optics Letters* **41**, 2907–2910 (July 2016).

[10] Savchenkov, A., Matsko, A., Liang, W., Ilchenko, V., Seidel, D., and Maleki, L., "Kerr frequency comb generation in overmoded resonators," *Optics Express* **20**(24), 27290–27298 (2012).

[11] Papp, S., Del'Haye, P., and Diddams, S., "Parametric seeding of a microresonator optical frequency comb," *Opt. Express* **21**(15), 17615–17624 (2013).

[12] Taheri, H., Eftekhar, A., Wiesenfeld, K., and Adibi, A., "Soliton formation in whispering-gallery-mode resonators via input phase modulation," *IEEE Photonics J.* **7**(2), 1–9 (2015).

[13] Lobanov, V., Lihachev, G., Pavlov, N., Cherenkov, A., Kippenberg, T., and Gorodetsky, M., "Harmonization of chaos into a soliton in Kerr frequency combs," *Optics Express* **24**(24), 27382–27394 (2016).

[14] Lobanov, V., Lihachev, G., and Gorodetsky, M., "Generation of platicons and frequency combs in optical microresonators with normal GVD by modulated pump," *Europhys. Lett.* **112**(5), 54008 (2015).

[15] Cole, D. C., Stone, J. R., Erkintalo, M., Yang, K. Y., Yi, X., Vahala, K. J., and Papp, S. B., "Kerr-microresonator solitons from a chirped background," *Optica* **5**(10), 1304–1310 (2018).

[16] Taheri, H., Matsko, A. B., Herr, T., and Sacha, K., "Dissipative discrete time crystals in a pump-modulated Kerr microcavity," *Communications Physics* **5**, 1–10 (June 2022).

[17] Taheri, H., *Ultrashort pulses in optical microresonators with Kerr nonlinearity*, PhD Thesis, Georgia Institute of Technology (2017).

[18] Obrzud, E., Lecomte, S., and Herr, T., "Temporal solitons in microresonators driven by optical pulses," *Nature Photonics* **11**, 600–607 (Sept. 2017).

[19] Strekalov, D. V. and Yu, N., "Generation of optical combs in a whispering gallery mode resonator from a bichromatic pump," *Phys. Rev. A* **79**, 041805 (Apr 2009).

[20] Hansson, T. and Wabnitz, S., "Bichromatically pumped microresonator frequency combs," *Phys. Rev. A* **90**, 013811 (Jul 2014).

[21] Taheri, H., Matsko, A., and Maleki, L., "Optical lattice trap for Kerr solitons," *The European Physical Journal D* **71**(6), 153 (2017).

[22] Fortier, T. M., Kirchner, M. S., Quinlan, F., Taylor, J., Bergquist, J., Rosenband, T., Lemke, N., Ludlow, A., Jiang, Y., Oates, C., et al., "Generation of ultrastable microwaves via optical frequency division," *Nature Photonics* **5**(7), 425 (2011).

[23] Taheri, H. and Matsko, A. B., "Dually-pumped Kerr microcombs for spectrally pure radio frequency signal generation and time-keeping," in [*Laser Resonators, Microresonators, and Beam Control XXI*], **10904**, 109040P, International Society for Optics and Photonics (Mar. 2019).

[24] Taheri, H., Matsko, A. B., Maleki, L., and Sacha, K., "All-optical dissipative discrete time crystals," *Nature Communications* **13**, 848 (Feb. 2022).

[25] Okawachi, Y., Yu, M., Luke, K., Carvalho, D. O., Ramelow, S., Farsi, A., Lipson, M., and Gaeta, A. L., "Dual-pumped degenerate Kerr oscillator in a silicon nitride microresonator," *Optics Letters* **40**, 5267–5270 (Nov. 2015).

[26] Okawachi, Y., Yu, M., Luke, K., Carvalho, D. O., Lipson, M., and Gaeta, A. L., "Quantum random number generator using a microresonator-based Kerr oscillator," *Optics Letters* **41**, 4194–4197 (Sept. 2016).

[27] Zhang, S., Silver, J. M., Bi, T., and Del'Haye, P., "Spectral extension and synchronization of microcombs in a single microresonator," *Nature Communications* **11**, 6384 (Dec. 2020).

[28] Moille, G., Perez, E. F., Stone, J. R., Rao, A., Lu, X., Rahman, T. S., Chembo, Y. K., and Srinivasan, K., "Ultra-broadband Kerr microcomb through soliton spectral translation," *Nature Communications* **12**, 7275 (Dec. 2021).

[29] Lu, Z., Chen, H.-J., Wang, W., Yao, L., Wang, Y., Yu, Y., Little, B. E., Chu, S. T., Gong, Q., Zhao, W., Yi, X., Xiao, Y.-F., and Zhang, W., "Synthesized soliton crystals," *Nature Communications* **12**, 3179 (May 2021).

[30] Taheri, H. and Matsko, A., "Crystallizing Kerr Cavity Pulse Peaks in a Timing Lattice," in [*Frontiers in Optics + Laser Science APS/DLS (2019), paper JTu3A.90*], Optical Society of America (Sept. 2019).

[31] Taheri, H., Matsko, A. B., Maleki, L., and Sacha, K., "Time Crystals in Optics," *Optics and Photonics News* , 9 (July/August 2022).

[32] Matsko, A. B. and Maleki, L., "Low threshold Kerr solitons," *Optics Letters* **48**, 715–718 (Feb. 2023).

[33] Trillo, S., Wabnitz, S., and Kennedy, T. A. B., "Nonlinear dynamics of dual-frequency-pumped multiwave mixing in optical fibers," *Physical Review A* **50**, 1732–1747 (Aug. 1994).

[34] Ceoldo, D., Bendahmane, A., Fatome, J., Millot, G., Hansson, T., Modotto, D., Wabnitz, S., and Kibler, B., "Multiple four-wave mixing and Kerr combs in a bichromatically pumped nonlinear fiber ring cavity," *Optics Letters* **41**, 5462–5465 (Dec. 2016).

[35] Chembo, Y. and Menyuk, C., "Spatiotemporal Lugiato-Lefever formalism for Kerr-comb generation in whispering-gallery-mode resonators," *Phys. Rev. A* **87**(5), 053852 (2013).

[36] Wabnitz, S., "Suppression of interactions in a phase-locked soliton optical memory," *Opt. Lett.* **18**(8), 601–603 (1993).

[37] Savchenkov, A., Matsko, A. B., and Taheri, H., "Independent Optical and Microwave Injection Locking of Kerr Frequency Combs by an Auxiliary Laser," in [*Frontiers in Optics + Laser Science 2022 (FIO, LS) (2022), Paper FTu6E.3*], FTu6E.3, Optica Publishing Group (Oct. 2022).